HHS Public Access

Author manuscript

*Mol Cancer Ther*. Author manuscript; available in PMC 2019 June 01.

Published in final edited form as:

*Mol Cancer Ther*. 2018 June ; 17(6): 1240–1250. doi:10.1158/1535-7163.MCT-17-1009.

# Gallium Maltolate Disrupts Tumor Iron Metabolism and Retards the Growth of Glioblastoma by Inhibiting Mitochondrial Function and Ribonucleotide Reductase

**Christopher R. Chitambar**[1], **Mona M. Al-Gizawiy**[2], **Hisham S. Alhajala**[1], **Kimberly R. Pechman**[3], **Janine P. Wereley**[1], **Robert Wujek**[2], **Paul A. Clark**[4], **John S. Kuo**[4], **William E. Antholine**[5], and **Kathleen M. Schmainda**[2,5]

[1]Department of Medicine, Medical College of Wisconsin, Milwaukee, Wisconsin

[2]Department of Radiology, Medical College of Wisconsin, Milwaukee, Wisconsin

[3]Department of Neurosurgery, Medical College of Wisconsin, Milwaukee, Wisconsin

[4]Department of Neurological Surgery, University of Wisconsin School of Medicine and Public Health, Madison, Wisconsin

[5]Department of Biophysics, Medical College of Wisconsin, Milwaukee, Wisconsin

## Abstract

Gallium, a metal with antineoplastic activity, binds transferrin (Tf) and enters tumor cells via Tf receptor1 (TfR1); it disrupts iron homeostasis leading to cell death. We hypothesized that TfR1 on brain microvascular endothelial cells (BMECs) would facilitate Tf-Ga transport into the brain enabling it to target TfR-bearing glioblastoma. We show that U-87 MG and D54 glioblastoma cell lines and multiple glioblastoma stem cell (GSCs) lines express TfRs and that their growth is inhibited by gallium maltolate (GaM) *in vitro.* After 24-h of incubation with GaM, cells displayed a loss of mitochondrial reserve capacity followed by a dose-dependent decrease in oxygen consumption and a decrease in the activity of the iron-dependent M2 subunit of ribonucleotide reductase (RRM2). Immunohistochemical staining of rat and human tumor-bearing brains showed that glioblastoma, but not normal glial cells, expressed TfR1 and RRM2 and that glioblastoma expressed greater levels of H- and L-ferritin than normal brain. In an orthotopic U-87 MG glioblastoma xenograft rat model, GaM retarded the growth of brain tumors relative to untreated control ($p=0.0159$) and reduced tumor mitotic figures ($p=0.045$). Tumors in GaM-treated animals displayed an upregulation of TfR1 expression relative to control animals thus indicating that gallium produced tumor iron deprivation. GaM also inhibited iron uptake and upregulated TfR1 expression in U-87 MG and D54 cells *in vitro.* We conclude that GaM enters the brain via TfR1 on BMECs and targets iron metabolism in glioblastoma *in vivo,* thus inhibiting tumor growth. Further development of novel gallium compounds for brain tumor treatment is warranted.

Corresponding author: Christopher R. Chitambar, MD, Division of Hematology and Oncology, Medical College of Wisconsin, 9200 W. Wisconsin Ave, Milwaukee, WI 53226, Phone: 414-805-4600, FAX: 414-805-4606, chitambr@mcw.edu.

Authors' Conflict of Interest: None

**Keywords**

glioblastoma; iron metabolism; gallium maltolate

## INTRODUCTION

Glioblastoma is a primary brain tumor with a dire prognosis. Despite treatment, the median survival of patients with this disease is 14.6 months; few patients survive beyond 2 years from diagnosis (1). The need to develop new therapies for this malignancy is obvious. In this regard, drugs directed at disrupting pathways involved in tumor growth are emerging (2). Recent evidence indicates that iron metabolism and iron-dependent tumor growth are promising targets for cancer treatment since tumor cells have an increased demand for iron to support ribonucleotide reductase activity and mitochondrial function (3). Moreover, iron is required for the activity of certain cyclins and for signaling through the mTOR and WNT pathways (4). A change in the balance of proteins that regulate the cellular intake, storage, and export of iron [transferrin receptor (TfR1), ferritin, and ferroportin, and hepcidin, respectively] in tumors leads to an expanded intracellular iron pool to support iron-dependent malignant cell growth (5). It has been shown that iron homeostasis and iron transport are altered in brain tumors relative to non-malignant cells (6,7). Iron, as Tf-Fe, enters the brain by TfRs present on the luminal surface of brain microvascular endothelial cells (BMECs) of the blood brain barrier (BBB) (8).

Gallium nitrate, a simple metal salt that targets iron metabolism, has clinical antineoplastic activity in bladder cancer and lymphoma (9). It shares certain chemical properties with iron that enables it's binding to transferrin (Tf), the transport protein for iron in the circulation (10). Gallium enters cells via TfR1-mediated endocytosis and blocks TfR1-mediated uptake of Tf-iron by cells (11). Within the cell, gallium disrupts iron-dependent tumor growth and induces cell death (11).

The antineoplastic activity of gallium nitrate has prompted the development of newer gallium compounds with complex ligand structures. These agents hold the promise of greater clinical efficacy and fewer side-effects (9). For example, gallium maltolate [(tris-hydroxy-2-methyl-4H-pyran-4-onato)gallium] (GaM) displays greater cytotoxicity than gallium nitrate in lymphoma cell lines and inhibits the growth of lymphoma cells that are resistant to the cytotoxicity of gallium nitrate (12). GaM also inhibits the growth of human T-cell lymphoma xenografts in nude mice confirming its anti-tumor activity both *in vitro* and *in vivo* (13).

Glioblastomas have a high requirement for iron (14). Since iron is taken up by cells through TfR1-mediated endocytosis and TfRs are highly expressed on the surface of glioblastoma cells (15), targeting cellular iron metabolism represents an attractive interventional strategy in glioblastoma therapy. Considering that gallium uses the transport and cellular uptake system for iron, we hypothesized that GaM can cross the BBB via TfRs on BMECs and target TfR-bearing glioblastoma cells. In this study, we show that GaM inhibits glioblastoma cell growth *in vitro* and *in vivo.* GaM's mechanisms of action include inhibition of cellular iron uptake, disruption of mitochondrial function, and inhibition of RRM2 activity in

glioblastoma cells. These findings open the door for further development of gallium-based compounds for glioblastoma treatment.

## Materials and Methods

### Materials

Gallium maltolate was provided by Titan Pharmaceuticals (South San Francisco, CA). Mouse anti-human TfR antibody (anti-CD71) and rabbit anti-rat TfR antibody were from Biogenex Laboratories (San Ramon, CA), and ABBIOTEC (San Diego, CA), respectively. Antibodies to RRM2, H- and L-ferritin, and TfR1 were purchased from Santa Cruz Biotechnology Inc (Santa Cruz, CA). Human Tf, 3-(4,5-Dimethylthiazol-2-yl)-2,5-diphenyltetrazolium bromide (MTT), oligomycin, carbonilcyanide 4-(trifluoromethoxy)phenylhydrazone (FCCP), and antimycin A were obtained from Sigma Chemical Company (St. Louis, MO). Alzet mini-pumps were obtained from Durect Corporation (Cupertino CA). $^{125}$I-Na and $^{55}FeCl_3$ were purchased from Perkin Elmer (Richmond, CA) and $^{125}$I-Tf and $^{55}$Fe-Tf were prepared as previously described (16).

### Cells

Tissue culture media and supplements were purchased from Life Technologies™ (Grand Island, NY, USA), unless stated otherwise. All cell lines used were validated at their point of origin. Human glioblastoma U-87 MG and D54 cell lines were obtained from American Type Culture Collection (ATCC®, Manassas, VA) and courtesy of Dr. D. Bigner, (Duke University Medical Center, Durham, NC), respectively. The U-87 MG cells were grown in MEM with Earle's salts fortified with 10% FBS, and supplemented with 1% sodium pyruvate and 0.1% gentamicin. D54 cells were grown in Improved MEM with Zn Option, fortified with 10% FBS, and supplemented with 0.1 % gentamicin. Human brain microvascular endothelial cells (BMECs) were a generous gift from Dr. Daniel Kosman (University of Buffalo, NY) and have been described previously (17). The glioblastoma stem cells (GSCs) were developed from human glioblastoma and were authenticated, as previously described (18). Experiments were conducted with GSC lines designated GSC-22, GSC-33, and GSC-44. These cells were maintained as neurospheres in a serum-free stem cell culture medium (18,19).

### Interaction of transferrin with GaM

The interaction of Tf with GaM was examined by UV-Vis (ultraviolet-visible) spectroscopy, as described by Harris and Pecoraro (10). Individual absorbance spectra of human Tf (12.5 μM) and GaM (25 μM) in water were obtained using a Varioskan Flash Spectral Scanning Multimode Reader (Thermo Fisher Scientific Inc. Waltham MA). Gallium maltolate was added incrementally to the Tf-containing cuvette to achieve final Ga concentrations of 25, 50, and 100 μM, respectively. Absorbance spectra were obtained at room temperature 10 min after the addition of each concentration of GaM to the cuvette.

### Cellular Tf binding and internalization

$^{125}$I-Tf specific binding to intact cells was measured as reported (20). For Tf internalization kinetics, cells were first incubated at 4°C to allow for $^{125}$I-Tf binding to cell surface TfR1

and then washed to remove unbound $^{125}$I-Tf. Warm medium (37°C) was added to cells to initiate TfR1 cycling and the fraction of acid-resistant, cell-associated $^{125}$I-Tf (representing internalized $^{125}$I-Tf) was measured at different time points.

### Cellular Proliferation

The effect of GaM on cell proliferation was measured by MTT cytotoxicity assay in 96-well microwell plates using an ELX 808 ultra microplate autoreader (Biotech Instruments, Winooski, VT) (12).

### Cellular Bioenergetics

The effect of GaM on cellular bioenergetic function was assessed by measuring the oxygen consumption rate (OCR, a measure of oxidative phosphorylation) in intact cells using a Seahorse 96XF Analyzer (Agilent Technologies, Santa Clara, CA), according to the manufacturer's directions. Seahorse XF analyzer methodology is reviewed by Dranka et *al* (21). D54 cells were plated in fresh medium in a 96-well plate ($10^4$ cells per well) and incubated without additives at 37°C in a $CO_2$ incubator. After 24 h of incubation, various concentrations of GaM were added to the wells and the incubation continued for an additional 24 h. The plate was transferred to an XF Analyzer and basal OCR was measured at three time-points. This was followed by sequential additions of oligomycin (1μg/ml), FCCP (1μM), and Antimycin A (10 μM).

### Electron Paramagnetic Resonance Spectroscopy (EPR)

X-band EPR spectra of U-87 MG cells incubated without or with 100 μM GaM for 24 h were obtained at 110 K with a Bruker EMX spectrometer located at the Nation Biomedical EPR Center at the Medical College of Wisconsin. EPR spectra were collected as described by us (22).

### Immunohistochemical analysis

TfR1, H-ferritin, L-ferritin, and RRM2 expression in normal brain and glioblastoma, and TfR1 expression in human brain microvascular endothelial cells were examined by immunohistochemical (IHC) staining of tissue samples from surgically resected glioblastoma tumors from patients or from animal experiments. Dead cells in tumor xenografts in GaM-treated animals were identified according to typical nuclear morphological changes: pyknosis (nuclear condensation), karyorhexis (nuclear fragmentation), and karyolysis (complete dissolution of the nuclear fragments). Percent dead cells were calculated out of a total of 1000 cells (viable and dead) counted. Human tissue was obtained from the Brain and Spinal Cord Tissue Bank of the Medical College of Wisconsin. IHC staining with specific primary antibodies was performed on a Dako Autostainer Plus Instrument using the Dako EnVision™ FLEX High pH Detection Kit protocol. Stained slides were visualized using a Nikon Eclipse 80i microscope equipped with a MicroPublisher 3.3 RTV color video camera (Q Imaging, Surrey, BC, Canada). The images were captured using NIS elements imaging software (Version 7.0, Nikon Instruments, Inc.).

### Western Blotting

Glioblastoma cells were analyzed for the expression of H-ferritin, L-ferritin, and RRM2 proteins by Western blotting using standard protocols. Protein bands on membranes were identified by primary antibodies followed by horseradish peroxidase-labeled secondary antibody. Membranes were developed in Enhanced Chemiluminescence Western blotting detection solution (Amersham, Arlington Heights, IL) and exposed to BioMax film for autoradiography.

### Animal experiments

The antineoplastic activity of GaM *in vivo* was examined in an intracranial U-87 MG xenograft rat model previously described by us (23). All protocols were approved by the Institutional Animal Care and Use Committee at the Medical College of Wisconsin.

Male athymic rats weighing approximately 250 g were anesthetized with an intraperitoneal injection of ketamine (60 mg/kg), acepromazine (0.9 mg/kg) and xylazine (6 mg/kg). Once appropriate anesthetic depth was ascertained, the head was immobilized in a stereotactic device. A 2.5 cm skin incision was made along the midline over the bregma and a 1-mm burr hole was drilled in the skull 1 mm anterior and 2 mm lateral to the bregma on the right side (24). Using a 10-μL gas-tight syringe (Hamilton Company, Reno Nevada), $2 \times 10^5$ U-87 MG cells were implanted into the right frontal lobe at a depth of 3 mm relative to the dural surface. The cells were continuously injected over 5 minutes, after which the needle was left stationary for 5 minutes and then slowly withdrawn over an additional 5 minutes. Afterwards, the skin was closed using 3M Vetbond™ Tissue Adhesive (3 M Animal Care Products, St. Paul, Minnesota).

Eight days following implantation of tumor cells, and after baseline MRI studies were performed, rats were anesthetized with 2% isoflurane. Using aseptic techniques, a small incision was made over the animal's neck and sharp dissection carried out down to the level of the jugular vein. The vein was skeletonized and each pump's drug release catheter was inserted and secured within the vessel lumen. A subcutaneous pocket was dissected free to hold the implanted Alzet minipump reservoir (Durect Corporation, Cupertino CA) and then the skin wound closed with sutures.

In clinical trials of gallium nitrate, the greatest antineoplastic activity and least toxicity was seen when the drug was administered by continuous intravenous infusion over 5 – 7 consecutive days (25). Based on this treatment schedule, GaM solution or saline control was administered intravenously through the subcutaneously implanted Alzet minipump to provide a steady delivery of GaM. A dose of 50 mg/kg/day was chosen because this was shown to be well tolerated without significant toxicity in rats (26).

Tumor response after 10 days of GaM therapy was assessed by MRI. The relative change in tumor size on MRI from initiation to completion of GaM treatment measured using RECIST V1.1 criteria, as used in the clinic (27). The change in cerebral blood volume (CBV) was measured as previously described (23).

### Statistical analysis

Analysis was conducted on the change in tumor size and CBV (day 18-day 8) between the control group and gallium-treated group of animals with a level of significance as p=0.05 (Mann-Whitney test).

### Cellular $^{55}$FeTf uptake

The effect of GaM on iron uptake by U87 and D54 cells was measured using $^{55}$FeTf, as previously described (28).

## Results

### Interaction of Tf with GaM, cellular TfR1 expression, and GaM cytotoxicity in glioblastoma cells

GaM is composed of three maltolate ligands bound to a central gallium atom in a propeller-like arrangement (Figure 1A) (29). At equimolar gallium concentrations, GaM proved to be more cytotoxic to D54 glioblastoma cells than gallium nitrate (Figure 1B). This suggests that, in contrast to gallium nitrate, lower concentrations of gallium as GaM are needed to inhibit tumor growth. Accordingly, GaM would be expected to display less toxicity to normal cells than gallium nitrate.

Early studies in animals confirmed that $^{67}$Ga citrate injected intravenously was bound entirely to Tf in the circulation (30) and that $^{67}$Ga uptake by cells occurred primarily through cell surface TfR1-mediated uptake of Tf-Ga (31). Since the binding of gallium to Tf alters the UV-Vis spectra for Tf (10), we examined whether GaM interacted with Tf by measuring changes in the individual UV-vis spectra of Tf, and GaM, and Tf mixed with GaM. As shown in Figure 1C, a progressive spectral shift was seen when GaM was added to Tf at different ligand to metal ratios, indicating an interaction between GaM and Tf. Whereas the major shift in the spectral peak suggestive of GaM-Tf interaction was seen at ≥280 nm, an increase in the absorbance of Tf at 240 – 250 nm was also noted when it was incubated with GaM. The latter may be due to the binding of Ga (independent of GaM) to Tf, as the formation of Tf-Ga is known to produce an increase in the absorbance of Tf at 242 nm (10). Hence, it is possible that in solution a small amount of Ga may dissociate from GaM to bind Tf.

Since Tf-Ga is preferentially taken up by TfR-bearing cells (11), TfR1 expression on these cells and on BMECs was assessed by $^{125}$I-Tf-TfR binding assay. As shown in Figure 1D, both D54 and U-87 MG cells expressed higher levels of specific Tf binding relative to BMECs which displayed 63–65% lower Tf binding. These results suggest that TfRs on glioblastoma cells can be preferentially targeted by Tf-Ga.

To mimic the treatment schedule of gallium nitrate used in clinical trials where the drug is administered continuous for 5 – 7 days (25), GaM was incubated with human glioblastoma cells for 5 days and the effect on cell proliferation examined. As shown in the dose-response curves in Figure 1E, GaM inhibited the growth of glioblastoma cells in a dose-dependent manner. In contrast, it was not cytotoxic to human BMECs, thus illustrating a significant

differential in GaM's cytotoxicity toward glioblastoma when compared to normal cells. Maltol alone did not inhibit cell proliferation (Figure 1E). GaM-induced cell death was confirmed by direct visualization of cells (Figure 1F). D54 cells incubated with 50 and 100 μM GaM for 48 and 96 h displayed morphologic changes of nuclear condensation and cellular fragmentation consistent with cell death (Figure 1F, panels b – f) compared with control cells which grew normally (Figure 1F, panels a and d). In other experiments, the GaM-containing culture medium was removed from the wells after 5 days of incubation and replaced with fresh medium lacking GaM. Incubation was then continued for an additional 5 days and cell growth assessed. Under these conditions, GaM-treated cells failed to regain their ability to proliferate. These latter results strongly suggest that the growth-inhibitory action of GaM is not reversible.

The $IC_{50}$ concentrations for GaM glioblastoma cells *in vitro* are relevant to gallium levels attainable *in vivo.* Tf has two metal-binding sites per molecule and its concentration in the blood is 25.25 – 45 μM. Under physiologic conditions, approximately one-third of Tf in the circulation is bound by iron thus leaving two-thirds of Tf available to bind Ga. Hence, gallium blood levels of 34 – 60 μM are possible if these remaining Tf metal-binding sites are occupied by gallium.

## GaM inhibits mitochondrial oxygen consumption

Several proteins of the citric acid cycle and the mitochondrial electron transport chain contain iron-sulfur clusters that are essential for their function. A decrease in cellular iron can therefore result in a loss of mitochondrial function (32,33). Since we have previously shown that gallium compounds can inhibit cellular iron uptake (28,34), we examined the effect of GaM on cellular respiration as a measure of mitochondrial function. In these experiments, intact cells were analyzed after they had been incubated with GaM concentrations that were not cytotoxic to cells over 24 h. As shown in Figure 2A, D54 cells incubated with 50 – 100 μM GaM for 24 h did not display evidence of cell death. However, as shown in Figure 2B, these cells displayed a progressive decrease in mitochondrial oxygen-dependent respiration (OCR) and a loss of mitochondrial reserve capacity after 24-h of incubation with increasing concentrations of GaM. Cells incubated with 25 μM GaM, displayed a loss of reserve capacity (also known as the spare respiratory capacity) without a decrease in OCR below baseline, thereby indicating that even low, non-cytotoxic concentrations of GaM affected the "fitness" of glioblastoma cells. At higher concentrations, GaM produced a decrease in OCR and reserve capacity. These results suggest that GaM decreases mitochondrial function as an early event before a decrease in cell proliferation or induction of cell death can be detected.

## GaM inhibits the iron-dependent activity of RRM2

Ribonucleotide reductase (RR) catalyzes the synthesis of deoxyribonucleotides, a rate-limiting step in DNA synthesis (35). As illustrated in Figure 3A, RR consists of two heterodimeric subunits M1 and M2 which are under the control of different genes (35). RRM2 expression increases as cells enter S-phase (36). RRM2 contains a binuclear iron center and an EPR-detectable tyrosyl free radical, both of which are essential for its activity (Figure 3A)(37). Cellular iron deprivation or blockade of iron incorporation into RRM2

inhibits RR enzymatic activity (38). Previously, we showed that gallium nitrate and Tf-Ga inhibit RRM2 activity in leukemia cells by : a) induction of cellular iron deprivation which limits iron availability to RRM2 (22,39), and b) direct action on enzymatic function which is independent of iron (40). To examine whether GaM interfered with RRM2 in glioblastoma cells, we measured the activity of the RRM2 tyrosyl radical by EPR spectroscopy in intact U-87 MG cells incubated with GaM for 24 hours. As shown in Figure 3B, the EPR signal in GaM-treated cells was reduced by approximately 65% relative to control cells. To determine whether this was due to a reduction in RRM2 protein, RRM2 expression in U-87 MG cells was analyzed by Western blotting after incubation with GaM for 24 h. In contrast to the reduction in the RRM2 EPR signal, we found that there was a 1.2 to 1.4-fold increase in RRM2 protein with 25 and 50 μM GaM (Figures 3C and 3D). Although the reason for this increase is not obvious, one possible explanation is that cells attempt to compensate for the GaM-induced loss of iron-dependent RR activity by increasing RRM2 protein production. Indeed, an amplification of the RRM2 gene occurs during the development of drug resistance to hydroxyurea, an agent that blocks RR activity by action on the tyrosyl radical of RRM2 (41). Collectively, these results indicate that GaM decreases the activity of iron-dependent RRM2 without reducing the synthesis of RRM2 protein.

## Expression of gallium-targeted iron proteins in normal brain and glioblastoma

To determine whether the expression of iron-related proteins in glioblastoma cells *in vitro* are relevant to glioblastoma *in vivo,* we examined normal and glioblastoma-containing brain tissue from rodent brains for TfR1 and ferritin and from human specimens for RRM2. Consistent with prior reports, we confirmed that TfRs were present on BMECs (Figure 4A) indicating that these receptors could serve as portals for GaM to traverse the BBB and enter the brain. Within the brain, TfR1 expression in glioblastoma cells was markedly increased relative to the adjacent normal brain (Figure 4B). The H- and L-subunits of the iron storage protein ferritin were also increased in glioblastoma (Figures 4C and 4D, respectively). Ferritin is composed of 24 subunits of H- and L-ferritin in proportions that differ in various cell types. L-subunit-rich ferritin exists in greater proportion in tissues (such as the liver) that store iron, while H-subunit-rich ferritin exists in greater proportion in metabolically active tissues such as the heart and malignant cells (42). As shown in Figure 4C and D, both H- and L-ferritin levels were increased in glioblastoma cells relative to normal brain. These findings are consistent with the studies of Schonberg *et al.* which showed that ferritin levels are elevated in glioblastoma (7).

Figure 4F shows that iron-containing RRM2 protein is highly expressed in human glioblastoma but not in normal brain (4E). Collectively, the data in Figure 4 strongly suggest that glioblastoma cells *in vivo* increase their expression of TfR1 and ferritin to acquire and store greater amounts of iron than the surrounding normal brain in order to support the activity of ribonucleotide reductase and other iron-dependent proteins necessary for tumor proliferation and viability.

## GaM retards the growth of glioblastoma in a rodent brain tumor model

Considering that GaM binds to Tf and inhibits the growth of glioblastoma cells *in vitro,* we hypothesized that GaM would enter the brain via TfR1 present on the BMECs of the BBB

and inhibit the growth of glioblastoma. Thus, we conducted a proof-of-principle experiment to examine the activity of GaM against glioblastoma *in vivo*. In the studies shown in Figure 5, GaM or saline solution (control) was administered to rats inoculated with U-87 MG glioblastoma xenografts in the brain. Treatment of animals with GaM or saline was initiated only after tumors were established in the brain. Tumor response to treatment was assessed by MR imaging and RECIST V1.1 criteria as used in the clinic (27). Figure 5A shows the pre-and post-treatment brain MRI from a representative experiment. Post-contrast T1 weighted images (T1+C) and MION CBV maps were obtained in a glioblastoma xenograft-bearing rat on days 8 and 18 for control (Figure 5A a,b,c,d) and a GaM-treated rat (Figure 5A e,f,g,h). In comparing the cohort of control versus GaM-treated animals, Figure 5B shows that GaM significantly inhibited the growth of glioblastoma relative to untreated controls. A decrease in CBV in GaM-treated animals was also noted (Figure 5C); while the difference in this parameter did not reach statistical significance, there was clearly a trend towards a reduction in CBV with gallium-treatment.

Tumors were examined for proliferation markers and TfR1 expression. Consistent with the antiproliferative activity of GaM, tumors from GaM-treated animals displayed a significant reduction in mitotic figures ($p = 0.043$) and mitotic index ($p = 0.045$) compared with untreated tumors (Figure 5 D, panels a and b). This finding is consistent with an *in vivo* inhibition of cellular proliferation by GaM in the glioblastoma xenograft and it clearly supports a cytostatic effect of GaM. In addition, GaM-treated tumors displayed a higher percentage of dead cells (37%) than untreated control tumors (24%). Although not significantly different, the observed trend in this parameter suggests that GaM exerts a cytotoxic effect that extends beyond inhibition of proliferation. The conclusion is supported by our prior studies which show that GaM induces apoptotic cell death in lymphoma cells (12), and by Figure 1F.

## GaM inhibits cellular iron uptake and upregulates TfR1 expression in glioblastoma in vitro and in vivo

The expression of TfR1 in tumors from control and GaM-treated animals was measured by IHC after completion of treatment. As shown in Figure 5E, TfR1 expression was markedly increased in GaM-treated tumors relative to control tumors. This finding is consistent with GaM-induced tumor iron-deprivation *in vivo* as we have previously shown that Tf-Ga blocks cellular iron uptake and upregulates TfR1 mRNA in human leukemic HL60 cells (43). However, to confirm that glioblastoma U-87 MG and D54 cells would respond to GaM in a similar fashion, we conducted additional experiments which showed that GaM inhibited the uptake of $^{55}$Fe-Tf (Figures 6A and 6B), and produced an upregulation of TfR1 in both these cell lines (Figure 6C). These results support our interpretation that the increase in tumor TfR1 expression in GaM-treated animals is secondary to GaM-induced tumor iron deprivation.

## GSCs express ferritin, TfR1, and RRM2, and are sensitive to the cytotoxicity of GaM

As an extension of our studies with U-87 MG and D54 cell lines, we investigated whether three previously described patient-derived GSC lines designated GSC-22, -33, and -44(19), expressed GaM-targeted iron-proteins and were sensitive to its cytotoxicity. Figure 6D

shows that all three GSC lines expressed immunoreactive H- and L-ferritin, and RRM2 proteins. Ligand-receptor binding and ligand internalization assays confirmed that TfR1 present on GSCs bound $^{125}$I-Tf (Figure 6E) and rapidly internalized it (Figure 6F). As shown in Figure 6G, the proliferation of these GSCs could be inhibited by GaM in a dose-dependent manner. Collectively, the experiments in studies in Figure 6 D–G indicate GSCs display highly functional TfR1 that can be targeted by GaM.

## Discussion

Our study is the first to show that a novel gallium compound, GaM, has antineoplastic activity against glioblastoma *in vivo*. We demonstrated that GaM inhibited the growth of glioblastoma cell lines *in vitro* and used MR imaging of the rat brain to measure the impact of GaM on the growth and vascularity of established glioblastoma brain tumor xenografts in live animals. These studies clearly show that GaM significantly retards the growth of tumors and reduces their relative blood volume over a ten-day period of treatment.

Early clinical studies with gallium-67 scans showed that $^{67}$Ga was taken up by brain tumors (44); additional studies revealed that the cellular uptake and cytotoxicity of gallium was enhanced by Tf (28,45). Consistent with earlier reports, we confirmed that TfRs were expressed on both BMECs and glioblastoma tumors in patients. These findings prompted us to investigate if TfRs could be exploited for the delivery of Tf-Ga to brain tumors.

The strategy of enhancing drug delivery to the brain by conjugating drugs or toxins to Tf or to anti-TfR1 antibodies to target BMEC TfRs has been reported by others (46). However, our approach is different in that we have taken advantage of the high-affinity binding of gallium to endogenous Tf in the circulation to deliver Ga to the brain. We propose that after crossing the BBB, Ga binds Tf in the brain leading to targeting of Tf-Ga to TfR-bearing glioblastoma cells. It is known that Tf in the normal brain is present in oligodendrocytes and is produced and secreted by the choroidal plexus (47). Furthermore, glioblastoma cells may also secrete Tf as an autocrine growth factor which may enable them to acquire iron for their growth. *In vitro* studies show that GSCs release Tf to culture medium (7). Thus, Tf in the tumor microenvironment intended to transport iron into TfR1-bearing glioblastoma cells could be hijacked by gallium to enhance its uptake by tumor cells. While our studies indicate that GaM penetrates the brain via TfR-mediated transport, it is possible that a variable amount of GaM may also cross the BBB independent of Tf; this is being investigated.

Whereas GaM retards the growth of glioblastoma, it needs to be determined whether gallium compounds will adversely impact on normal brain function. In this regard, it is encouraging to note that central nervous system toxicity was not reported in Phase I and II clinical trials of gallium nitrate (25,26). Also, we did not observe neurological deficits in the rats treated with GaM. An important consideration is that normal glial cells do not express TfRs *in vivo* (8). Thus, gallium is likely to be taken up by TfR1-expressing glioblastoma cells but not by normal glial tissue. However, neuronal cells do express TfRs (8) and could be targeted by Tf-Ga; but whether this would lead to neuronal toxicity remains to be determined. Collectively, both preclinical and clinical studies suggest a therapeutic index for gallium in

which gallium compounds could display antitumor efficacy at concentrations unlikely to affect normal brain cells.

We show that GaM inhibits iron-dependent RRM2 and mitochondrial function. An important point in considering RRM2 as a target in glioblastoma is that normal brain cells do not proliferate *in vivo* and thus would not be expected to express RRM2. In contrast, glioblastoma being a high-grade proliferating brain tumor would be expected to express RRM2. This was confirmed in our studies comparing the expression of immunoreactive RRM2 protein in glioblastoma versus normal brain. Hence GaM, as an inhibitor of iron-dependent RRM2 activity, would be expected to block DNA synthesis in glioblastoma cells but not in normal brain cells.

Whereas gallium-induced inhibition of RRM2 in itself would be sufficient to inhibit the proliferation of glioblastoma brain tumors, other iron-dependent mechanisms beyond RR could be targeted by gallium. Thus, we focused on GaM's action on the mitochondria. We hypothesized that iron-sulfur cluster-containing proteins of the citric acid cycle and mitochondrial electronic transport chain could be prime targets for disruption by GaM and that this could result in a block in energy production and cell death. We discovered that even at non-cytotoxic concentrations, GaM produced loss of cellular reserve capacity (RC) in glioblastoma cells. This finding indicates that one of the initial mechanisms of action of GaM on the mitochondria is a loss of its spare respiratory capacity; this could decrease a cell's ability to cope with an energy demand (48). At higher concentrations, GaM further suppressed mitochondrial function as evidenced by a dose-dependent decrease cellular OCR and RC. This this effect undoubtedly contributes to Ga-induced cell death.

Central to gallium's mechanisms of action is its ability to disrupt of cellular iron metabolism at several levels (11). Consistent with this mechanism, we found that tumors in GaM-treated rats increased their expression of TfR1. Cellular iron deprivation produces an upregulation of TfR synthesis due to the enhanced interaction of cytoplasmic iron regulatory proteins-1 and -2 (IRPs-1,-2) with iron regulatory elements (IREs) present on the 3' untranslated region of the TfR mRNA (49). In support of this mechanism, we demonstrated that GaM inhibited iron uptake by U-87 MG and D54 cells *in vitro* and that this resulted in an increase in cellular TfR expression. Collectively, our studies strongly support tumor iron-deprivation as one of the mechanisms of action of GaM against glioblastoma *in vivo.*

In summary, our results show for the first time that a gallium compound that perturbs tumor iron homeostasis has potential in the therapy of glioblastoma brain tumors. Our animal studies serve as proof-of-principle that GaM can enter the rodent brain and retard the growth of glioblastoma tumors; this builds the foundation for additional research. Future studies will investigate the efficacy of gallium compounds alone and in combination with other drugs in GSC-derived orthotopic xenograft models. These studies will determine the optimum dose and treatment schedule for gallium compounds and their impact on survival. It is envisioned that such preclinical studies will lead to GaM-based clinical trials in glioblastoma.

## Acknowledgments

Funding: This work was supported by the Thomas A. and Lorraine M. Rosenberg Award for Translational Cancer Research from the Froedtert Hospital Foundation and the Medical College of Wisconsin Cancer Center (CRC); National Institutes of Health National Biomedical EPR Center Grant EB0011980 (WEA), and National Cancer Institute at the National Institutes of Health (grant number R01 CA 082500) and the MCW Advancing Healthier Wisconsin Research Program (KMS).

## References

1. Stupp R, Hegi ME, Mason WP, van den Bent MJ, Taphoorn MJ, Janzer RC, et al. Effects of radiotherapy with concomitant and adjuvant temozolomide versus radiotherapy alone on survival in glioblastoma in a randomised phase III study: 5-year analysis of the EORTC-NCIC trial. Lancet Oncol. 2009; 10:459–66. [PubMed: 19269895]
2. Ohka F, Natsume A, Wakabayashi T. Current trends in targeted therapies for glioblastoma multiforme. Neurol Res Int. 2012; 2012:878425. [PubMed: 22530127]
3. Richardson DR, Kalinowski DS, Lau S, Jansson PJ, Lovejoy DB. Cancer cell iron metabolism and the development of potent iron chelators as anti-tumour agents. Biochim Biophys Acta. 2009; 1790:702–17. [PubMed: 18485918]
4. Torti SV, Torti FM. Iron and cancer: more ore to be mined. Nat Rev Cancer. 2013; 13:342–55. [PubMed: 23594855]
5. Pinnix ZK, Miller LD, Wang W, D'Agostino R Jr, Kute T, Willingham MC, et al. Ferroportin and iron regulation in breast cancer progression and prognosis. Sci Transl Med. 2010; 2:43ra56.
6. Hanninen MM, Haapasalo J, Haapasalo H, Fleming RE, Britton RS, Bacon BR, et al. Expression of iron-related genes in human brain and brain tumors. BMC Neurosci. 2009; 10:36. [PubMed: 19386095]
7. Schonberg DL, Miller TE, Wu Q, Flavahan WA, Das NK, Hale JS, et al. Preferential Iron Trafficking Characterizes Glioblastoma Stem-like Cells. Cancer Cell. 2015; 28:441–55. [PubMed: 26461092]
8. Moos T, Rosengren NT, Skjorringe T, Morgan EH. Iron trafficking inside the brain. J Neurochem. 2007; 103:1730–40. [PubMed: 17953660]
9. Chitambar CR. Gallium-containing anticancer compounds. Future Med Chem. 2012; 4:1257–72. [PubMed: 22800370]
10. Harris WR, Pecoraro VL. Thermodynamic binding constants for gallium transferrin. Biochemistry. 1983; 22:292–9. [PubMed: 6402006]
11. Chitambar CR. Gallium and its competing roles with iron in biological systems. Biochim Biophys Acta. 2016; 1863:2044–53. [PubMed: 27150508]
12. Chitambar CR, Purpi DP, Woodliff J, Yang M, Wereley JP. Development of gallium compounds for treatment of lymphoma: Gallium maltolate, a novel hydroxypyrone gallium compound induces apoptosis and circumvents lymphoma cell resistance to gallium nitrate. J Pharmacol Exp Ther. 2007; 322:1228–36. [PubMed: 17600139]
13. Wu X, Wang TW, Lessmann GM, Saleh J, Liu X, Chitambar CR, et al. Gallium Maltolate Inhibits Human Cutaneous T-Cell Lymphoma Tumor Development in Mice. J Invest Dermatol. 2014; 135:877–44. [PubMed: 25371972]
14. Legendre C, Garcion E. Iron metabolism: a double-edged sword in the resistance of glioblastoma to therapies. Trends Endocrinol Metab. 2015; 26:322–31. [PubMed: 25936466]
15. Voth B, Nagasawa DT, Pelargos PE, Chung LK, Ung N, Gopen Q, et al. Transferrin receptors and glioblastoma multiforme: Current findings and potential for treatment. J Clin Neurosci. 2015; 22:1071–6. [PubMed: 25891893]
16. Chitambar CR, Wereley JP. Transferrin receptor-dependent and -independent iron transport in gallium-resistant human lymphoid leukemic cells. Blood. 1998; 91:4686–93. [PubMed: 9616166]
17. Stins MF, Badger J, Sik KK. Bacterial invasion and transcytosis in transfected human brain microvascular endothelial cells. Microb Pathog. 2001; 30:19–28. [PubMed: 11162182]

18. Clark PA, Iida M, Treisman DM, Kalluri H, Ezhilan S, Zorniak M, et al. Activation of multiple ERBB family receptors mediates glioblastoma cancer stem-like cell resistance to EGFR-targeted inhibition. Neoplasia. 2012; 14:420–8. [PubMed: 22745588]
19. Zorniak M, Clark PA, Leeper HE, Tipping MD, Francis DM, Kozak KR, et al. Differential expression of 2',3'-cyclic-nucleotide 3'-phosphodiesterase and neural lineage markers correlate with glioblastoma xenograft infiltration and patient survival. Clin Cancer Res. 2012; 18:3628–36. [PubMed: 22589395]
20. Klausner RD, van Renswoude J, Ashwell G, Kempf C, Schecter AN, Dean A, et al. Receptor-mediated endocytosis of transferrin in K562 cells. J Biol Chem. 1983; 258:4715–24. [PubMed: 6300098]
21. Dranka BP, Benavides GA, Diers AR, Giordano S, Zelickson BR, Reily C, et al. Assessing bioenergetic function in response to oxidative stress by metabolic profiling. Free Radic Biol Med. 2011; 51:1621–35. [PubMed: 21872656]
22. Narasimhan J, Antholine WE, Chitambar CR. Effect of gallium on the tyrosyl radical of the iron-dependent M2 subunit of ribonucleotide reductase. Biochem Pharmacol. 1992; 44:2403–8. [PubMed: 1335254]
23. Pechman KR, Donohoe DL, Bedekar DP, Kurpad SN, Hoffmann RG, Schmainda KM. Characterization of bevacizumab dose response relationship in U87 brain tumors using magnetic resonance imaging measures of enhancing tumor volume and relative cerebral blood volume. J Neurooncol. 2011; 105:233–9. [PubMed: 21533524]
24. Pechman KR, Donohoe DL, Bedekar DP, Kurpad SN, Schmainda KM. Evaluation of combined bevacizumab plus irinotecan therapy in brain tumors using magnetic resonance imaging measures of relative cerebral blood volume. Magn Reson Med. 2012; 68:1266–72. [PubMed: 22213469]
25. Warrell RP Jr, Coonley CJ, Straus DJ, Young CW. Treatment of patients with advanced malignant lymphoma using gallium nitrate administered as a seven-day continuous infusion. Cancer. 1983; 51:1982–7. [PubMed: 6839291]
26. Foster BJ, Clagett-Carr K, Hoth D, Leyland-Jones B. Gallium nitrate: The second metal with clinical activity. Cancer Treat Rep. 1988; 70:1311–9.
27. Eisenhauer EA, Therasse P, Bogaerts J, Schwartz LH, Sargent D, Ford R, et al. New response evaluation criteria in solid tumours: revised RECIST guideline (version 1.1). Eur J Cancer. 2009; 45:228–47. [PubMed: 19097774]
28. Chitambar CR, Seligman PA. Effects of different transferrin forms on transferrin receptor expression, iron uptake and cellular proliferation of human leukemic HL60 cells: Mechanisms responsible for the specific cytotoxicity of transferrin-gallium. J Clin Invest. 1986; 78:1538–46. [PubMed: 3465751]
29. Bernstein LR, Tanner T, Godfrey C, Noll B. Chemistry and pharmacokinetics of gallium maltolate, a compound with high oral gallium bioavailability. Metal-Based Drugs. 2000; 7:33–47. [PubMed: 18475921]
30. Vallabhajosula SR, Harwig JF, Siemsen JK, Wolf W. Radiogallium localization in tumors:Blood binding and transport and the role of transferrin. J Nucl Med. 1980; 21:650–6. [PubMed: 7391839]
31. Larson SM, Rasey JS, Allen DR, Nelson NJ, Grunbaum Z, Harp GD, et al. Common pathway for tumor cell uptake of Gallium-67 and Iron-59 via a transferrin receptor. J Natl Cancer Inst. 1980; 64:41–53. [PubMed: 6243376]
32. Oexle H, Gnaiger E, Weiss G. Iron-dependent changes in cellular energy metabolism: influence on citric acid cycle and oxidative phosphorylation. Biochim Biophys Acta. 1999; 1413:99–107. [PubMed: 10556622]
33. Yoon YS, Byun HO, Cho H, Kim BK, Yoon G. Complex II defect via down-regulation of iron-sulfur subunit induces mitochondrial dysfunction and cell cycle delay in iron chelation-induced senescence-associated growth arrest. J Biol Chem. 2003; 278:51577–86. [PubMed: 14512425]
34. Chitambar CR, Narasimhan J. Targeting iron-dependent DNA synthesis with gallium and transferrin-gallium. Pathobiology. 1991; 59:3–10. [PubMed: 1645976]
35. Aye Y, Li M, Long MJ, Weiss RS. Ribonucleotide reductase and cancer: biological mechanisms and targeted therapies. Oncogene. 2014; 34:2011–21. [PubMed: 24909171]

36. Eriksson S, Gräslund A, Skog S, Thelander L, Tribukait B. Cell cycle-dependent regulation of mammalian ribonucleotide reductase. The S phase-correlated increase in subunit M2 is regulated by de novo protein synthesis. J Biol Chem. 1984; 259:11695–700. [PubMed: 6090444]
37. Gräslund A, Sahlin M, Sjöberg B-M. The tyrosyl free radical in ribonucleotide reductase. Environ Health Perspect. 1985; 64:139–49. [PubMed: 3007085]
38. Nyholm S, Mann GJ, Johansson AG, Bergeron RJ, Gräslund A, Thelander L. Role of ribonucleotide reductase in inhibition of mammalian cell growth by potent iron chelators. J Biol Chem. 1993; 268:26200–5. [PubMed: 8253740]
39. Chitambar CR, Matthaeus WG, Antholine WE, Graff K, O'Brien WJ. Inhibition of leukemic HL60 cell growth by transferrin-gallium: Effects on ribonucleotide reductase and demonstration of drug synergy with hydroxyurea. Blood. 1988; 72:1930–6. [PubMed: 3058232]
40. Chitambar CR, Narasimhan J, Guy J, Sem DS, O'Brien WJ. Inhibition of ribonucleotide reductase by gallium in murine leukemic L1210 cells. Cancer Res. 1991; 51:6199–201. [PubMed: 1933878]
41. Wright JA, Alam TG, McClarty GA, Tagger AY, Thelander L. Altered expression of ribonucleotide reductase and role of M2 gene amplification in hydroxyurea-resistant hamster, mouse, rat and human cell lines. Somatic Cell Mol Genet. 1987; 13:155–65.
42. Torti FM, Torti SV. Regulation of ferritin genes and protein. Blood. 2002; 99:3505–16. [PubMed: 11986201]
43. Haq RU, Chitambar CR. Modulation of transferrin receptor mRNA by transferrin-gallium in human myeloid HL60 cells and lymphoid CCRF-CEM cells. Biochem J. 1993; 294:873–7. [PubMed: 8379943]
44. Waxman AD, Siemsen JK, Lee GC, Wolfstein RS, Moser L. Reliability of gallium brain scanning in the detection and differentiation of central nervous system lesions. Radiology. 1975; 116:675–8. [PubMed: 1153779]
45. Harris AW, Sephton RG. Transferrin promotion of $^{67}$Ga and $^{59}$Fe uptake by cultured mouse myeloma cells. Cancer Res. 1977; 37:3634–8. [PubMed: 561654]
46. McCarthy RC, Kosman DJ. Mechanistic analysis of iron accumulation by endothelial cells of the BBB. Biometals. 2012; 25:665–75. [PubMed: 22434419]
47. Leitner DF, Connor JR. Functional roles of transferrin in the brain. Biochim Biophys Acta. 2012; 1820:393–402. [PubMed: 22138408]
48. Nicholls, DG., Ferguson, SJ., editors. Bioenergetics. 4. 2013. Respiratory Chains; p. 91-157.
49. Lane DJ, Merlot AM, Huang ML, Bae DH, Jansson PJ, Sahni S, et al. Cellular iron uptake, trafficking and metabolism: Key molecules and mechanisms and their roles in disease. Biochim Biophys Acta. 2015; 1853:1130–44. [PubMed: 25661197]

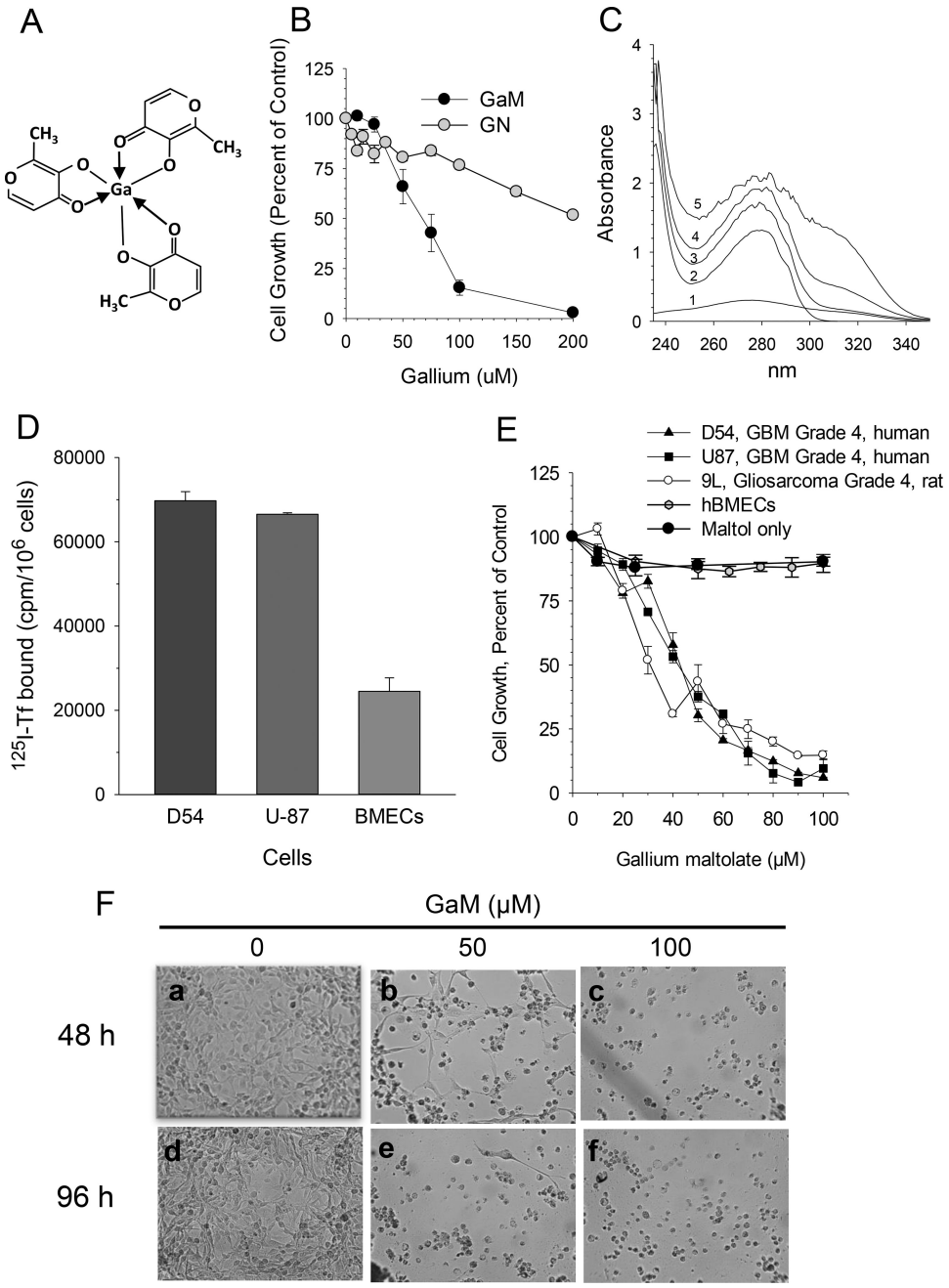


**Figure 1.**

GaM interaction with transferrin (Tf), Tf binding to cells, and effect of GaM on cell growth. A. Chemical structure of gallium maltolate. B. Comparison of the growth-inhibitory effects of gallium maltolate (GaM) and gallium nitrate (GN). D54 cells were incubated with equimolar concentrations of gallium as either GaM or GN. Cell proliferation was measured by MTT assay after 72-h of incubation. Values shown represent the means +/− S.E. (n = 3). C. GaM forms complexes with Tf *in vitro*. UV-visual spectra of 100 μM GaM (spectrum 1), 12.5 μM Tf (spectrum 2), and 12.5 μM Tf incubated with 12, 50, or 100 μM GaM (spectra 3, 4, and 5, respectively). Spectra were obtained at room temperature after a 30 minute

incubation of Tf with GaM. D. TfR expression on glioblastoma cells and brain microvascular endothelial cells (BMECs). Specific $^{125}$I-Tf binding to TfR1 on intact cells is shown. E. GaM inhibits the growth of glioblastoma cell lines but not human brain microvascular endothelial cells (hBMECs). Maltol alone does not inhibit D54 cell growth. Cell growth was measured by MTT assay after a 5-day incubation of cells with GaM. Values shown represent means ± S.E. (n=3). F. Gallium maltolate induces cell death. Photomicrographs showing morphologic changes consistent with GaM-induced cell death in D54 cells incubated without or with GaM for 48 h (panels a, b and c) or 96 h (panels d, e, and f), respectively.

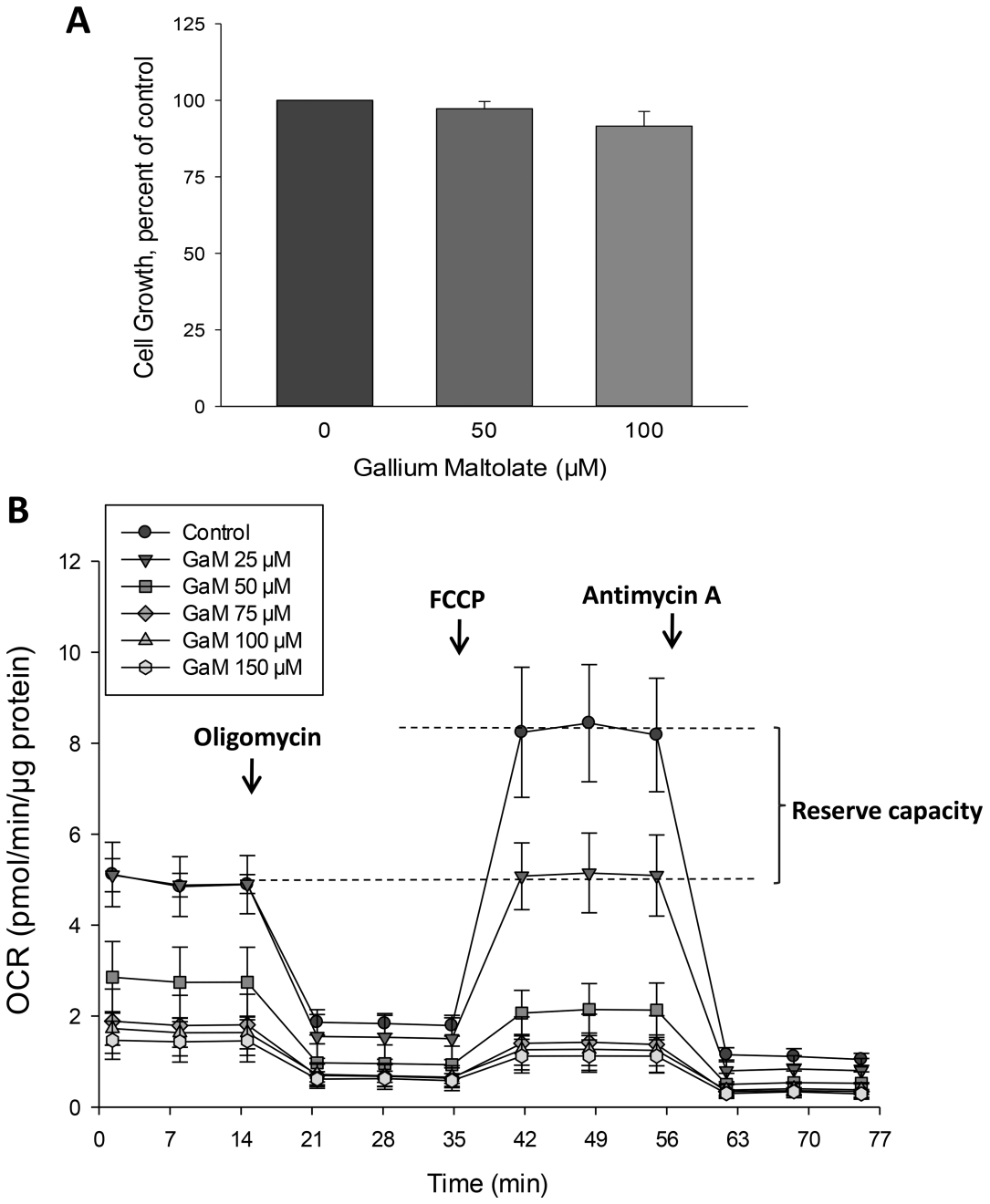


**Figure 2.**

GaM inhibits mitochondrial bioenergetics. A. Effect of GaM on cellular proliferation after a 24-incubation. Cellular proliferation in D54 cells was measured by MTT assay. B. Effect of GaM on mitochondrial bioenergetics in D54 cells after a 24-h incubation. Cellular oxygen consumption rate (OCR) was measured by a Seahorse 96XF Analyzer, as described under Methods.

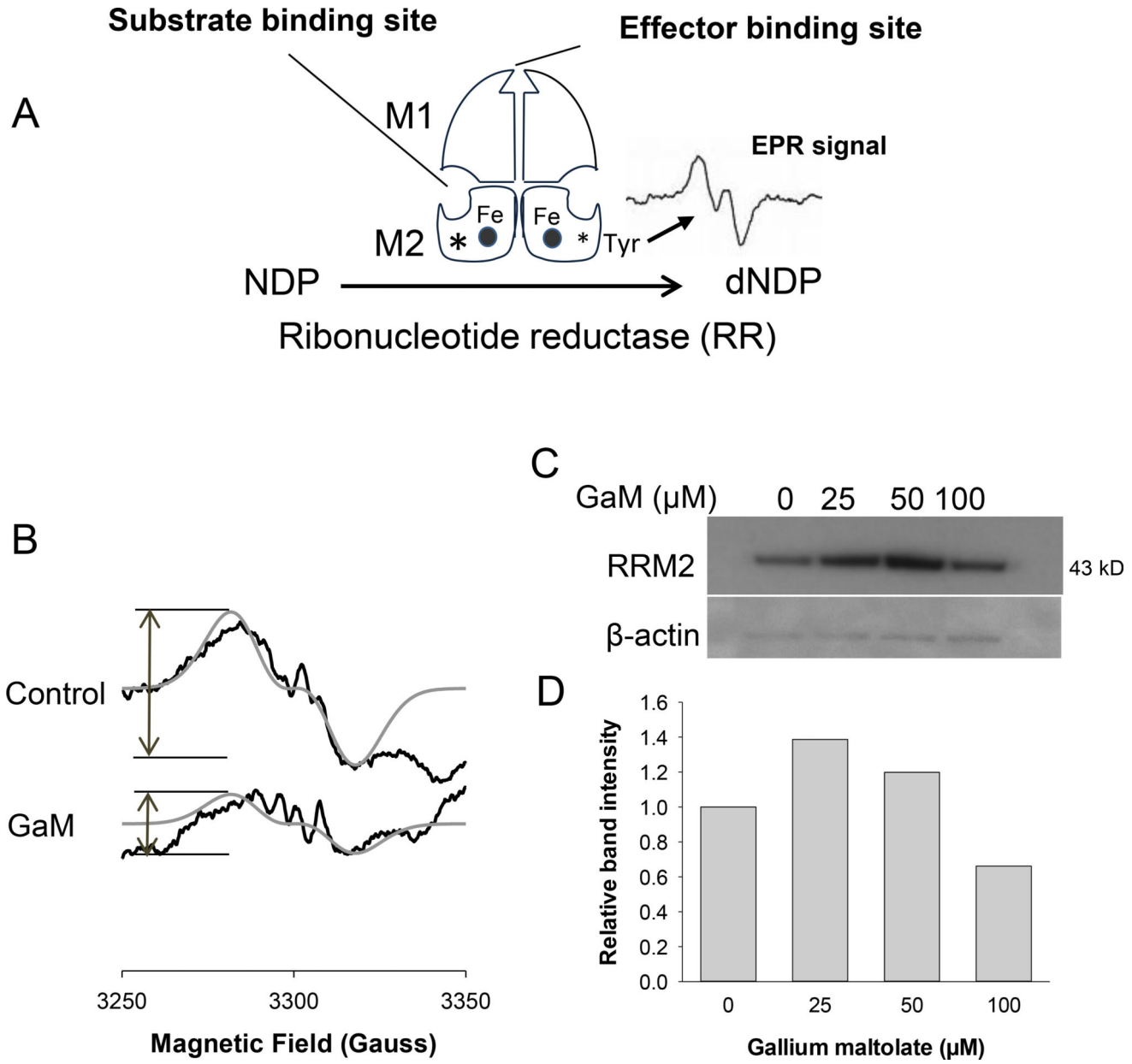


**Figure 3.**

Effect of GaM on the iron-dependent M2 subunit of ribonucleotide reductase (RRM2). A. Figure showing the components of RR. B. GaM inhibits the EPR signal of the RRM2 tyrosyl radical. Intact U-87 MG cells incubated without or with 100 μM GaM for 24 h were analyzed by EPR spectroscopy. EPR spectra of the control and GaM-treated cells (black line); simulated spectra for the tyrosyl radical (gray line), g-2.005, A=53.2 MHz (19 G) for single proton using Easyspin. C. RRM2 protein levels in cells incubated with GaM. Cells were analyzed by Western blotting after 24 h incubation with increasing concentrations of GaM. D. Densitometry of the bands shown in C.

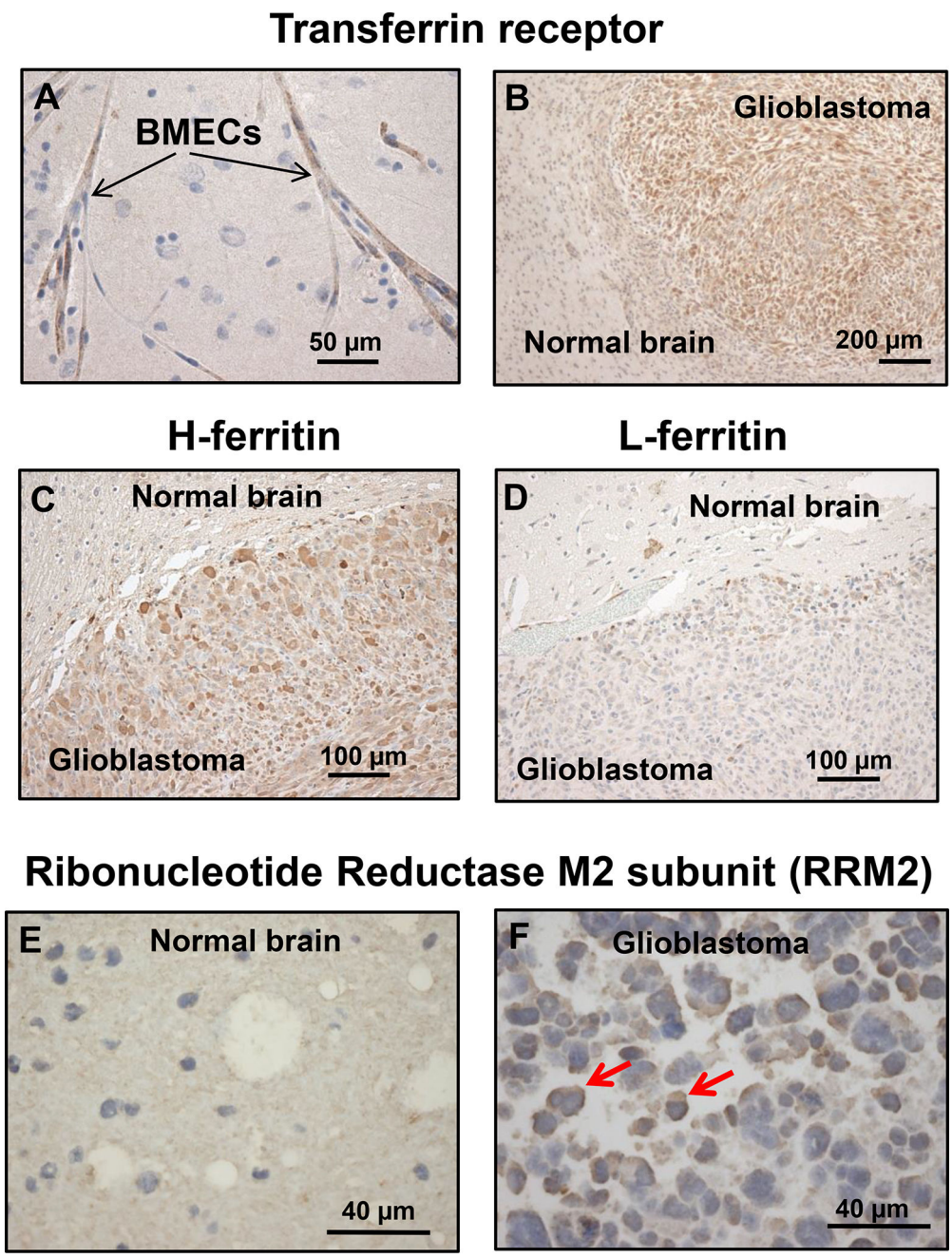


**Figure 4.**

Transferrin, transferrin receptor1 (TfR1), and ribonucleotide reductase M2 proteins in glioblastoma and normal brain. Proteins were identified by immunohistochemical (IHC) staining. A. TfR1 in human brain microvascular endothelial cells (BMECs). B. TfR1 in a U-87 MG glioblastoma xenograft inoculated in rat brain. C and D. H- and L-ferritin in a U-87 MG glioblastoma xenograft inoculated in rat brain. E. RRM2 in human normal brain tissue removed therapeutically from a patient with a seizure disorder. F. RRM2 in glioblastoma removed from a patient. Red arrows show increased brown staining of RRM2 protein. Increased RRM2 protein is also seen in other malignant cells.

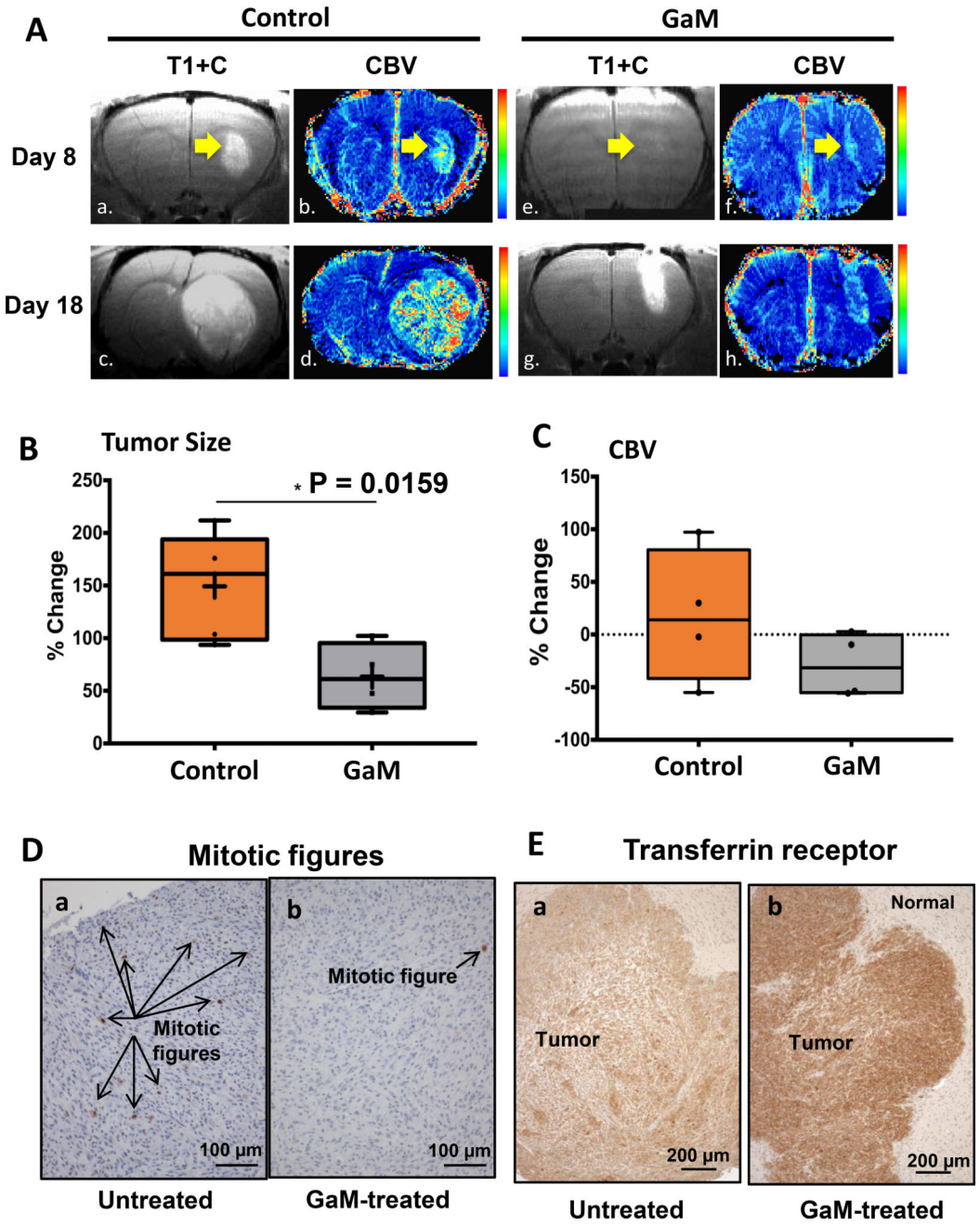


**Figure 5.**

GaM retards the growth of glioblastoma and alters tumor TfR1 expression *in vivo*. A. MR imaging of the brain. Figure shows the post-contrast (T1+C) images and cerebral blood volume (CBV) maps for a control (left panels: a,b,c,d respectively) and a GaM-treated rat (right panel: e,f,g,h) at each imaging time point (day 8 and day 18). B. GaM significantly retards the increase in tumor size. Comparison of the percent change in tumor growth (day 8 to 16) in the total control (n=5) and GaM-treated (n=4) population. C. GaM reduces the change in relative cerebral volume (day 8 to 16). D. Mitotic figures are significantly reduced in GaM-treated tumors. E. Transferrin receptors (brown staining) are increased in GaM-

treated tumors. Tumors from control (untreated) and GaM-treated animals were harvested after completion of treatment and analyzed by IHC for TfR1 expression. Photomicrographs from representative animals are shown.

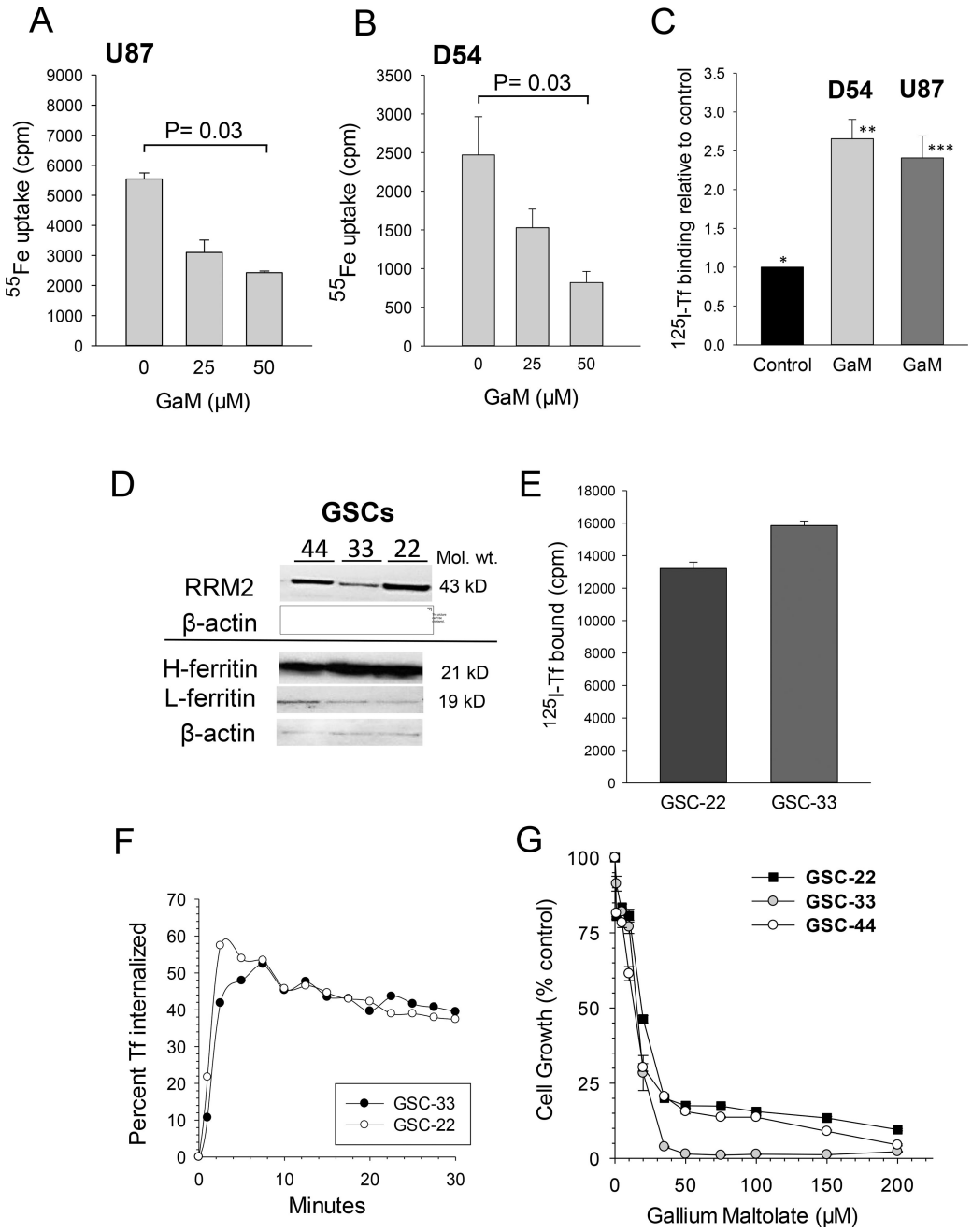


**Figure 6.**

A, B, and C. *GaM inhibits cellular iron uptake and upregulates TfR1 expression in glioblastoma cells*. A and B. $^{55}$Fe up by U-87 MG (A) and D54 cells (B) was measured after cells had been incubated with $^{55}$FeTf for 3 hours in the presence increasing concentrations of GaM. Values shown are means ± S.E. of $^{55}$Fe uptake per 5 × $10^5$ cells. C. TfR1 expression in U-87 MG and D54 cells was measured by $^{125}$I-Tf binding after a 24 h incubation of cells with 50 μM GaM. Values shown are means ± S.E. of specific $^{125}$I-Tf bound per $10^6$ cells. Differences between control cells (*, no GaM) and GaM-treated D54 (**) and U87 (***) cells are highly significant (p= 0.002, n = 6, for D54, and p = 0.008, n =

3, for U87 cells). D, E, and F. *Gallium-targeted iron proteins in glioblastoma stem cells (GSCs).* D. Western blot showing ribonucleotide reductase M2 (RRM2) and H- and L-ferritin in GSCs-44, -3, and -22. E. TfR1 expression on GSC-22 and -33. E. TfR1-mediated internalization kinetics of cell surface TfR-bound $^{125}$I-Tf. F. Inhibition of GSC cell growth by GaM. Cell proliferation was measured by MTT assay after a 120 h incubation of cells with GaM.